Agricultural Water Management 97 (2010) 1039–1050

Contents lists available at ScienceDirect

Agricultural Water Management

journal homepage: www.elsevier.com/locate/agwat

Sensitivity of groundwater recharge under irrigated agriculture to changes in climate, CO_2 concentrations and canopy structure

Darren L. Ficklin[a], Eike Luedeling[a,b], Minghua Zhang[a,*]

[a] Department of Land, Air and Water Resources, University of California, Davis, CA 95616, USA
[b] World Agroforestry Center (ICRAF), United Nations Avenue, Nairobi, Kenya

ARTICLE INFO

Article history:
Received 11 September 2009
Accepted 7 February 2010
Available online 12 March 2010

Keywords:
Hydrology
Groundwater
Recharge
Vadose zone
Climate change
HYDRUS
Agriculture

ABSTRACT

Estimating groundwater recharge in response to increased atmospheric CO_2 concentration and climate change is critical for future management of agricultural water resources in arid or semi-arid regions. Based on climate projections from the Intergovernmental Panel on Climate Change, this study quantified groundwater recharge under irrigated agriculture in response to variations of atmospheric CO_2 concentrations (550 and 970 ppm) and average daily temperature (+1.1 and +6.4 °C compared to current conditions). HYDRUS 1D, a model used to simulate water movement in unsaturated, partially saturated, or fully saturated porous media, was used to simulate the impact of climate change on vadose zone hydrologic processes and groundwater recharge for three typical crop sites (alfalfa, almonds and tomatoes) in the San Joaquin watershed in California. Plant growth with the consideration of elevated atmospheric CO_2 concentration was simulated using the heat unit theory. A modified version of the Penman–Monteith equation was used to account for the effects of elevated atmospheric CO_2 concentration. Irrigation amount and timing was based on crop potential evapotranspiration. The results of this study suggest that increases in atmospheric CO_2 and average daily temperature may have significant effects on groundwater recharge. Increasing temperature caused a temporal shift in plant growth patterns and redistributed evapotranspiration and irrigation water use earlier in the growing season resulting in a decrease in groundwater recharge under alfalfa and almonds and an increase under tomatoes. Elevating atmospheric CO_2 concentrations generally decreased groundwater recharge for all crops due to decreased evapotranspiration resulting in decreased irrigation water use. Increasing average daily temperature by 1.1 and 6.4 °C and atmospheric CO_2 concentration to 550 and 970 ppm led to a decrease in cumulative groundwater recharge for most scenarios. Overall, the results indicate that groundwater recharge may be very sensitive to potential future climate changes.

1. Introduction

In arid and semi-regions, estimating aquifer recharge is important for determining water resource availability and assessing aquifer vulnerability to pollutants. Recharge rates are dependent on the amount of water available at the land surface, which can vary temporally and spatially depending on climatic factors such as precipitation and evapotranspiration and land use factors such as crop type (Scanlon et al., 2002). In agriculturally dominated regions such as the semi-arid Central Valley of California, the estimation of recharge becomes complicated by irrigation, potentially creating new source areas of recharge while simultaneously depleting groundwater resources. In such regions, accurate estimates of recharge and evapotranspiration are important for management of scarce water resources.

While it is widely accepted that increased atmospheric concentrations of greenhouse gases, such as CO_2, are the leading causes of climate change (IPCC, 2007), few studies have assessed the change that increased CO_2 concentrations and climate changes will have on the hydrologic cycle via changes in plant growth and transpiration (e.g., Eckhardt and Ulbrich, 2003; Ficklin et al., 2009). Increased atmospheric CO_2 concentration has two main effects on plant evapotranspiration: [1] decreased stomatal conductance due to a reduced level of stomatal openings and [2] increased rate of leaf area growth from increased cell expansion. The influence of increasing CO_2 concentrations on leaf conductance was reviewed by Morison (1987). Morison found that at CO_2 concentrations between 330 and 660 ppm, a doubling in CO_2 concentration resulted, on average, in a 40% linear reduction in leaf stomatal conductance for 80 plant observations. Pritchard et al. (1999) wrote a review on the effects of

* Corresponding author. Tel.: +1 530 752 4953; fax: +1 530 752 5262.
E-mail address: mhzhang@ucdavis.edu (M. Zhang).

0378-3774/$ – see front matter © 2010 Elsevier B.V. All rights reserved.
doi:10.1016/j.agwat.2010.02.009

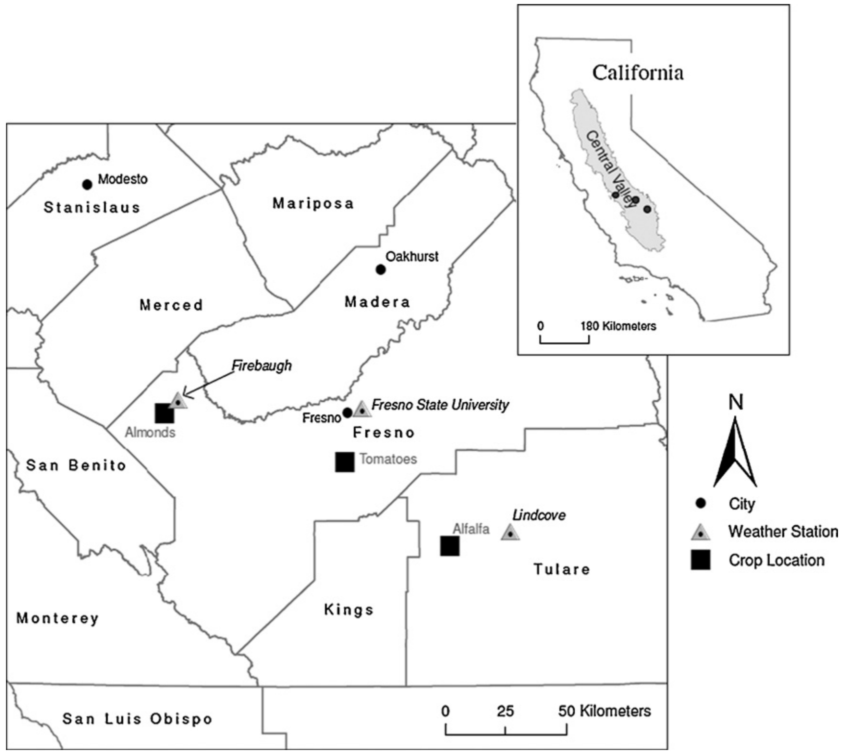

Fig. 1. Map of study area showing the locations of the three representative crops.

increasing atmospheric CO_2 on plant leaf area. Their work indicates that an average net increase in leaf area per plant of 24% is expected with a doubling of atmospheric CO_2. In highly agricultural regions such as California's Central Valley, changes in plant transpiration and growth may significantly alter the hydrologic cycle, as evapotranspiration is a significant source of water loss.

California's water storage system can be thought of as three reservoir systems: [1] Sierra Nevada snowpack, [2] collection of dams, lakes and conveyance systems for surface water, and [3] groundwater storage. Development of California's surface water storage system has slowed significantly, while groundwater usage is currently increasing and will continue to increase in the future at a strong pace (California DWR, 2003). With the continual decline of Sierra Nevada snow pack (which feeds the surface water reservoirs) due to climate change (e.g., Maurer, 2007) and increases in agricultural production and population growth, groundwater will increasingly become important as a major source of California's water needs. Therefore, it is extremely important to assess the effects that increases in atmospheric CO_2 concentration and climate change may have on groundwater resources within these regions.

Over the last several years, researchers have begun to estimate potential impacts of climate change on groundwater resources throughout the world (e.g., Scibek et al., 2007; Wessolek and Asseng, 2006). These studies differ in modeling methodologies, climate scenarios, results of groundwater sensitivities to climate, and interpretation of results. Other studies have used paleo-recharge estimation using tracer methods (Zuppi and Sacchi, 2004; Yin et al., 2008). The objective of this study is to conduct forward numerical modeling using HYDRUS 1D (Šimunek et al., 2005) to evaluate the sensitivity of elevated atmospheric CO_2 concentration, climate change and varying canopy structure of three case study crops on groundwater recharge in California. This research has implications on current and future water resource guidance of groundwater recharge.

2. Study sites

California's Central Valley covers approximately 100,000 square kilometers and is one of the most productive agricultural regions in the world (NASS, 2009) (Fig. 1). The state's agriculture is dominated by high-value specialty crops such as lettuce, tomatoes, fruits, almonds, walnuts and grapes. In 2005, California's total agricultural value was over $31 billion per year, ranking first in the United States. California produces 99% of the almonds and 95% of the processing tomatoes grown in the United States (CA-DOF, 2007). California also produces over 21% of the United States' milk and, consequently, alfalfa is the state's highest acreage crop. California is also the leading alfalfa-producing state in the United States (CARD, 2009). Most of the agriculture within California's Central Valley relies heavily on irrigation from surface water diversions and groundwater pumping.

This study was confined to the San Joaquin Valley in California (Fig. 1). The San Joaquin Valley has a typical Mediterranean climate. The maximum temperature during the hottest months of the year (June–August) may exceed 40 °C. Average temperatures in July and January in the northern part of the valley are 23.9 and 7.2 °C, respectively; whereas, average temperatures in July and January in the southern part of the valley are 29.9 and 8.3 °C, respectively. More than 80% of the precipitation occurs in winter, with an annual average of 36.3 cm in the northern part of the valley and 14.5 cm in the southern part of the valley (Vossen, 2008). The region is relatively flat due to alluvial deposits from several California rivers (Stanislaus, Tuolumne, Merced, Fresno, San Joaquin, Kings, Kern and Kaweah).

3. Materials and methods

3.1. Description of the numerical model

The numerical model package HYDRUS 1D (Šimunek et al., 2005) was used to simulate the processes of water flow, root water

Table 1
Soil hydraulic properties of the representative soil profiles.

Soil Name	Layer	Depth (cm)	AWC	Sand (%)	Silt (%)	Clay (%)	Bd (g/cm^3)	K_s (cm/d)	θ_s (cm^3/cm^3)	θ_r (cm^3/cm^3)	α (1/cm)	n
Hanford (tomatoes)	1	30.48	0.14	67.26	20.24	12.5	1.58	29.62	0.3673	0.0451	0.0325	1.42
	2	127	0.13	67.26	20.24	12.5	1.6	27.28	0.362	0.0445	0.0335	1.41
	3	152.4	0.1	67.26	20.24	12.5	1.61	26.17	0.3593	0.0442	0.034	1.4
Panoche (almonds)	1	17.78	0.16	35.45	33.55	31	1.52	5.46	0.4039	0.0752	0.0128	1.4
	2	101.6	0.17	34.68	37.82	27.5	1.53	5.47	0.3933	0.0706	0.0112	1.44
	3	152.4	0.14	55.84	17.66	26.5	1.58	11.14	0.3863	0.0648	0.0223	1.3
	4	177.8	0.12	65.91	19.09	15	1.63	19.99	0.3577	0.0472	0.0319	1.36
Yettem (alfalfa)	1	35.56	0.16	65.39	23.11	11.5	1.56	31.05	0.3683	0.0431	0.0317	1.42
	2	177.8	0.13	65.39	23.11	11.5	1.61	25.42	0.3556	0.0417	0.0343	1.39

uptake, root growth and evaporation from the soil surface in one-dimensional variably saturated media. It was assumed that the air phase does not affect liquid flow processes and that the water flow due to thermal gradients is negligible. HYDRUS 1D approximates the solution to the Richards Equation (Richards, 1931), the governing equation of water flow:

$$\frac{\partial\theta}{\partial t} = \frac{\partial}{\partial z}\left[K\left(\frac{\partial h}{\partial z}+1\right)\right] - S \tag{1}$$

where θ is the volumetric water content, t is time, h is the water pressure head, z is the spatial coordinate and K is the unsaturated hydraulic conductivity, a function of the saturated hydraulic conductivity (K_s) and water content. S represents a sink term, which accounts for the uptake of soil-water by vegetation (Feddes et al., 1978):

$$S(h) = \alpha(h)S_p \tag{2}$$

where $S(h)$ is the water uptake rate, $\alpha(h)$ is a water stress response function ($0 \leq \alpha \leq 1$) that describes the reduction in uptake under drought conditions and S_p is the potential water uptake rate. $S(h)$ is partitioned into each layer according to the depth-specific root density. For $\alpha(h)$, the functional form developed by Feddes et al. (1978) was used:

$$\alpha(h) = \begin{cases} \dfrac{h-h_4}{h_3-h_4} & h_4 < h \leq h_3 \\ 1 & h_3 < h \leq h_2 \\ \dfrac{h-h_1}{h_2-h_1} & h_2 < h \leq h_1 \\ 0 & h \leq h_4 \text{ or } h > h_1 \end{cases} \tag{3}$$

where h_1, h_2, h_3 and h_4 are the threshold parameters such that uptake is at the potential rate when the pressure head is between h_2 and h_3, drops off linearly when $h > h_2$ or $h < h_3$, and becomes zero when $h \leq h_4$ or $h > h_1$. These values are crop-specific and were taken from the database contained in HYDRUS 1D and the literature (Šimunek et al., 2005).

The van Genuchten (1980) and Mualem (1976) representations for unsaturated hydraulic properties used in this study are given by:

$$\theta(h) = \begin{cases} \theta_r + \dfrac{\theta_s-\theta_r}{\left[1+\left|\alpha h\right|^n\right]^m} & h < 0 \\ \theta_s & h \geq 0 \end{cases} \tag{4}$$

$$K(h) = K_s S_e^l\left[1-\left(1-S_e^{1/m}\right)^m\right]^2 \tag{5}$$

$$m = 1 - \frac{1}{n} \qquad n > 1 \tag{6}$$

where S_e is the effective saturation:

$$S_e = \frac{\theta(h)-\theta_r}{\theta_s-\theta_r} \tag{7}$$

and where θ_r is the residual soil-water content, θ_s is the saturated soil-water content, K_s is the saturated hydraulic conductivity, α is the air entry parameter, n is the pore size distribution parameter and l is the pore connectivity parameter. The parameters α, n and l are empirical coefficients that determine the shape of the hydraulic functions. l was set to 0.5, a common assumption based on the work of Mualem (1976). No hydrologic data were available for site-specific calibration, so the model was not calibrated to present conditions. The goal of this research is to test the sensitivity of groundwater recharge to climate change and calibration was not needed.

3.2. Description of the physical model

Three representative crop sites were chosen based on county crop acreage and value within California. First, the counties that produced the highest quantities of the crops chosen for this study were determined. Tulare County is one of the leading producers of alfalfa (total value of \$158 million in 2008) and Fresno County is the leading producer of almonds and tomatoes (total value of \$483 and \$348 million in 2008, respectively) (CARD, 2009). The alfalfa crop used in this study is a perennial crop and the modeled portion of the growth period is one cycle of harvest, which is approximately 31 days during the summer months. Second, through literature review and GIS land use/soil map overlays, representative soil profiles for all crops in their respective counties were determined (Fig. 1). Based on the spatial data layers, the Hanford and Panoche soil series were two of the largest soil types in Fresno County (10 and 8% of Fresno County, respectively). The Yettem soil series was one of the largest soil types in Tulare County (7% of Tulare County). Agricultural land comprises over 80% of the total land use on these soil series. Therefore, these soil series were used as inputs for the vadose zone model. It is important to note that the soil profiles are representative profiles for the respective crops and may spatially vary throughout the county. Therefore, spatial extrapolation of groundwater recharge results should be done with caution. The soil profile characteristics are listed in Table 1.

HYDRUS 1D requires specifying the soil hydraulic parameters θ_r, θ_s, α, K_s and l. Soil property data was extracted from the 1:24,000 Soil Survey Geographic (SSURGO) database (USDA, 2007). The soil hydraulic parameters were generated with ROSETTA (Schaap et al., 2001) using the soil physical properties of sand percentage, silt percentage, clay percentage and bulk density from SSURGO. ROSETTA is a pedotransfer function software package that uses a neural network model to predict soil hydraulic parameters from soil texture and related data. ROSETTA contains a hierarchy of pedotransfer functions that can be used depending on soil characterization data that are available. Soil hydraulic and physical properties of the four sites are shown in Table 1. It was assumed that the soil in each layer is homogenous and isotropic. The bottom of the model domain was set as the bottom of the soil profile.

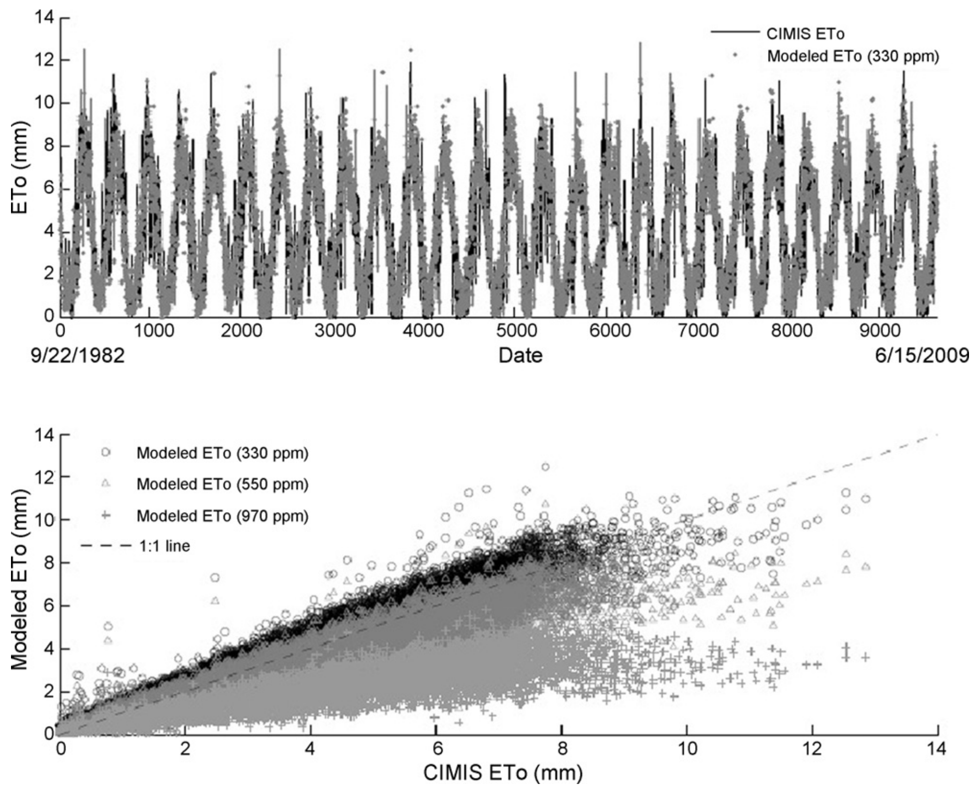

Fig. 2. Comparison of modeled and CIMIS potential evapotranspiration with multiple CO_2 concentrations at the Davis, CA CIMIS site.

4. Boundary conditions

The upper boundary condition in HYDRUS 1D was defined as an atmospheric boundary condition with surface runoff, where the potential flux across the surface boundary is controlled by external conditions such as precipitation, potential evapotranspiration (ETo) and leaf area index (LAI) (Neuman et al., 1975). Implementing the atmospheric boundary condition required specifying daily irrigation and precipitation rates, as well as daily ETo and LAI. The lower boundary condition was defined as a free drainage boundary, with the bottom of the soil profile as a zero-gradient boundary condition (Šimunek et al., 2005). This condition is appropriate for situations where the water table lies below the domain of interest (Šimunek et al., 2005), a reasonable assumption for this study. The bottom water flux was assumed to be equal to groundwater recharge.

A variable time stepping routine with maximum and minimum time steps of 1.44 min ($\sim 1 \times 10^{-3}$ days) and 0.02 min (1×10^{-5} days), respectively, was used for all simulations based on HYDRUS 1D. One representative growing season was simulated for all climate change sensitivity scenarios. For example, the tomato growing season started and ended on April 1st and August 31st, respectively. The reference and 6 climate and CO_2 scenarios were then simulated for this timeframe using respective climate, ETo, LAI, irrigation amount and scheduling and root growth for each climate scenario.

4.1. Reference climate

Observed climate data used for reference and climate change scenarios were extracted from the California Irrigation Management Information System (CIMIS) weather stations of Firebaugh, Fresno State University and Lindcove (Fig. 1). This dataset includes precipitation, solar radiation, temperature (air and dew point), relative humidity and wind speed. Reference ETo was calculated from the observed climate data using the modified Penman–Monteith method discussed in Section 4.5 (Penman, 1948; Monteith, 1965). Fig. 2 shows CIMIS ETo data compared with modeled ETo data. Precipitation was used as an upper boundary condition for all scenarios.

The reference climate simulation consisted of the respective CIMIS stations' mean daily temperature (air and dew point), wind speed, solar radiation and relative humidity for the length of the available weather records. Each CIMIS station had no less than 20 years of climate data. Precipitation data were taken from an average precipitation year (neither wet nor dry). The precipitation year of 2001 was selected for the Fresno and Firebaugh CIMIS stations and 2003 for the Lindcove CIMIS station. An average precipitation year was determined by summing the yearly precipitation amounts and choosing the closest yearly amount to the mean and standard deviation of the entire precipitation record. The climate data was then used to produce ETo, LAI and irrigation amount and scheduling.

4.2. Generation of climate change scenarios

The different scenarios selected for this study are based on the IPCC Special Report on Emission Scenarios (SRES) (2001) and The Physical Science Basis (2007). The reports describe divergent projections of future atmospheric CO_2 concentration and climate and their underlying uncertainty. Depending on the greenhouse gas emission scenario, atmospheric CO_2 is expected to increase from the current concentration of 330 ppm to between approximately 550 and 970 ppm by the end of the 21st century (IPCC, 2001). The scenarios with the highest (A1FI scenario: 970 ppm by year 2100) and lowest (B1 scenario: 550 ppm by year 2100) projected CO_2 concentrations were chosen for this study. The A1FI scenario assumes a future world of very rapid economic growth, global population that peaks in mid-century and declines thereafter and rapid introduction of new and more efficient, but fossil intensive technologies. The B1 scenario, in contrast, corresponds to a future of low economic

Table 2
Scenarios for climate change simulations.

Scenario	CO_2 Conc. (ppm)	Temperature (°C)
Reference	330	+0
1	330	+1.1
2	330	+6.4
3	550	+0
4	550	+1.1
5	970	+0
6	970	+6.4

growth and fossil-fuel usage. GCMs vary in their predictions of rainfall for California over the 21st century, and therefore precipitation change was not considered. Table 2 shows all climate change scenarios used in the simulations. All climate change scenarios were run for one crop growing season. Each climate change component (CO_2 concentration and temperature) was increased for the entire growing season. For example, a scenario may have a 550 ppm CO_2 concentration and an increase of average daily temperature by 1.1 °C, both of which are simulated for the entire growing season. The results were summarized by total cumulative recharge and its percent change with respect to the present-day reference simulation. *T*-tests were done to determine if the climate scenarios and the present-day scenarios were statistically different from each other.

4.3. Irrigation

Irrigation amount and scheduling were determined using the Basic Irrigation Scheduling (BIS) program developed by Snyder et al. (2007). BIS calculates daily crop coefficient values (K_c) and crop evapotranspiration based on calculated ETo rates. It uses a water budget method approach for determining irrigation amount and scheduling, which depends on soil, plant and climate data. Full details of BIS can be found in Snyder et al. (2007). In the simulation, irrigation water was applied to alfalfa in 4-day increments and almonds and tomatoes in 7-day increments. Initial soil-water deficit for all crops was assumed to be 2 cm. This value is the default value in BIS and assumes that crops are pre-irrigated before planting (a common method in California) or that the growing season follows a wet winter (Snyder et al., 2007). Irrigation application efficiency was set at the default value of 80% in BIS to account for runoff and evaporation from the soil surface. This irrigation efficiency value represents a wide range of irrigation methods (Howell, 2003). Irrigation application amounts were input into HYDRUS 1D as precipitation, since the model considers precipitation and irrigation as the same boundary condition. Irrigation amount and scheduling for each crop type can be found in the Supplementary Tables S1–S3.

4.4. Leaf area index

LAI is needed as an upper boundary condition for all scenarios. LAI is the ratio of the upper leaf surface of vegetation divided by the surface area of the land on which the vegetation grows. The LAI modeled in this study differs from 'effective LAI', an estimate of LAI which takes into account the lumping and randomness of foliage elements in the vegetation. LAI was modeled using the heat unit theory (Boswell, 1926; Magoon and Culpepper, 1932), which has proven to be a reliable predictor of crop growth for various crop types (e.g., Cross and Zuber, 1972; Guerra et al., 2004). The heat unit theory hypothesizes that plants have heat requirements that can be quantified and correlated with time-to-maturity. A plant is assumed to only grow when the mean daily temperature exceeds the base temperature. For example, tomatoes have a base growth temperature of 10 °C. If the mean temperature for a particular day is 22 °C, the heat units accumulated on that day are 22 − 10 = 12 heat units. Knowing the planting date, maturity or harvest date, base temperature and mean daily temperatures, the total number of heat units required to bring a crop to maturity (also known as Potential Heat Units) can be calculated. It is assumed that all temperatures above the base temperature accelerate crop development. The heat unit accumulation for a given day is calculated as:

$$\mathrm{HU} = T_{ave} - T_{base} \qquad \text{when } T_{ave} > T_{base} \tag{8}$$

where HU is the number of heat units for a particular day, T_{ave} is the daily mean temperature and T_{base} is the base temperature for the plant. The total number of heat units required for a plant to reach maturity is:

$$\mathrm{PHU} = \sum_{d=1}^{m} \mathrm{HU} \tag{9}$$

where PHU is the potential number of heat units, HU is the number of heat units accumulated on day d where $d = 1$ at the planting date and m is the number of days for the plant to reach maturity. To calculate potential heat units, the number of days for a plant to reach maturity must be known. Potential heat units were calculated based on average planting and harvest dates and average temperature from the crops' representative CIMIS station. The plant growth characteristics are summarized in Table 3.

LAI was calculated using the heat unit theory for all scenarios with the methods developed by Williams et al. (1989). Full details can be found in Nietsch et al. (2005). In the initial period of plant growth, leaf area development is controlled by the optimal leaf area development curve:

$$fr_{\mathrm{LAImx}} = \frac{fr_{\mathrm{PHU}}}{fr_{\mathrm{PHU}} + \exp(l_1 - l_2 \times fr_{\mathrm{PHU}})} \tag{10}$$

where fr_{LAImx} is the fraction of the plant's maximum LAI corresponding to the fraction of PHUs for the plant, fr_{PHU} is the fraction of PHUs accumulated for the plant on a given day, l_1 and l_2 are shape coefficients of the leaf area development curve. The fraction

Table 3
Growth and evapotranspiration characteristics for the reference crops.

Crop	Plant date	Harvest date	Base temperature (°C)	Potential heat units	Crop coefficient (K_c)				Maximum rooting depth (m)	$g_{l,mx}$ (m/s)	$\Delta_{\mathrm{LAICO_2}}$	$\Delta_{\mathrm{glCO_2}}$
Alfalfa (cycle)	20-June	20-July	4	1939	0.4	1.15	1.15	0.4	0.6	0.01	0.26[a]	−0.42[b]
Almonds	1-March	15-October	10	4479	0.55	1.05	1.05	0.65	3.5	0.0036	0.35[c]	−0.33[d]
Tomatoes	1-April	31-August	10	1763	0.3	1.1	1.1	0.65	2	0.008	0.32[e]	−0.21[f]

[a] Aranjuelo et al. (2009).
[b] Aranjuelo et al. (2006).
[c] Medlyn et al. (2001).
[d] Pritchard et al. (1999).
[e] Pallas (1965).
[f] Willits and Peet (1989).

of potential heat units accumulated on a given day is:

$$fr_{\mathrm{PHU}} = \frac{\sum_{i=1}^{d} \mathrm{HU}_i}{\mathrm{PHU}} \tag{11}$$

The shape coefficients are calculated by solving Eq. (10) for two known points ($fr_{\mathrm{LAI},1}, fr_{\mathrm{PHU},1}$) and ($fr_{\mathrm{LAI},2}, fr_{\mathrm{PHU},2}$):

$$l_1 = \ln\left[\frac{fr_{\mathrm{PHU},1}}{fr_{\mathrm{LAI},1}} - fr_{\mathrm{PHU},1}\right] + l_2 \times fr_{\mathrm{PHU},1} \tag{12}$$

$$l_2 = \frac{\ln[(fr_{\mathrm{PHU},1}/fr_{\mathrm{LAI},1}) - fr_{\mathrm{PHU},}] - \ln[(fr_{\mathrm{PHU},2}/fr_{\mathrm{LAI},2}) - fr_{\mathrm{PHU},2}]}{fr_{\mathrm{PHU},2} - fr_{\mathrm{PHU},1}} \tag{13}$$

where l_1 is the first shape coefficient, l_2 is the second shape coefficient, $fr_{\mathrm{PHU},1}$ is the fraction of the growing season corresponding to the first point on the optimal leaf area development curve, $fr_{\mathrm{LAI},1}$ is the fraction of the maximum LAI corresponding to the first point on the optimal leaf area development curve, $fr_{\mathrm{PHU},2}$ is the fraction of the growing season corresponding to the second point on the optimal leaf area development curve and $fr_{\mathrm{LAI},2}$ is the fraction of the maximum LAI corresponding to the second point on the optimal leaf area development curve. The coefficients $fr_{\mathrm{PHU},1}, fr_{\mathrm{PHU},2}, fr_{\mathrm{LAI},1}$ and $fr_{\mathrm{LAI},2}$ are known for various crops and were taken from the EPIC crop database (Williams et al., 1989).

The amount of LAI generated on day i is:

$$\Delta\mathrm{LAI}_i = (fr_{\mathrm{LAImx},i} - fr_{\mathrm{LAImx},i-1}) \times \mathrm{LAI}_{\mathrm{mx}} \times (1 - \exp(5 \times (\mathrm{LAI}_{i-1} - \mathrm{LAI}_{\mathrm{mx}}))) \tag{14}$$

where $\Delta\mathrm{LAI}_i$ is the leaf area added on day i, LAI_i and LAI_{i-1} are the leaf area indices for day i and $i-1$, respectively, $fr_{\mathrm{LAImx},i}$ and $fr_{\mathrm{LAImx},i-1}$ are the fraction of the plant's maximum LAI calculated with Eq. (10) for day i and $i-1$, respectively, and LAImx is the maximum LAI for the plant, taken from the EPIC crop database (Williams et al., 1989). The perennial almond crops used in this study were assumed to be at full maturity. LAI for day i is:

$$\mathrm{LAI}_i = \mathrm{LAI}_{i-1} + \Delta\mathrm{LAI}_i \tag{15}$$

To achieve a reasonable simulation of LAI, it was assumed that the crop was never under stress due to lack of water or nutrients. It is likely that in the future, growers would continue to achieve the highest yield possible with additions of water and nutrients. It is beyond the scope of this study, however, to determine whether there would be enough irrigation water available and that nutrients would still be economically feasible to add to crops.

LAI increases as elevated CO_2 concentrations were incorporated into the LAI model by adjusting the LAI to allow for the effects of increased atmospheric CO_2 concentration based on a similar method as Easterling et al. (1992):

$$\mathrm{LAI}(CO_2) = \mathrm{LAI} \times \left((1 - \Delta_{\mathrm{LAICO_2}}) + \Delta_{\mathrm{LAICO_2}}\left(\frac{CO_2}{330}\right)\right) \tag{16}$$

where $\mathrm{LAI}(CO_2)$ is the LAI modified to account for the effects of CO_2, $\Delta_{\mathrm{LAICO_2}}$ is the LAI percentage change for a doubling of CO_2 (%) and CO_2 is the concentration of CO_2 in the atmosphere (ppm). It was assumed that the effect of CO_2 on LAI is linear.

4.5. Potential evapotranspiration

ETo is needed as an upper boundary condition for all scenarios. This study used a modified version of the Penman–Monteith ETo model (Penman, 1948; Monteith, 1965). The Penman–Monteith model is:

$$\lambda E = \frac{\Delta \times (H_{\mathrm{net}} - G) + \rho_{\mathrm{air}} \times c_p \times [e_z^o - e_z]/r_a}{\Delta + \gamma \times (1 + r_c/r_a)} \tag{17}$$

where λE is the latent heat flux density (MJ m^{-2} d^{-1}), E is the depth rate of evaporation (mm d^{-1}), Δ is the slope of the saturation vapor pressure–temperature curve, H_{net} is the net radiation (MJ m^{-2} d^{-1}), G is the heat flux density to the ground (MJ m^{-2} d^{-1}; assumed to be zero for all simulations (Hatfield et al., 1984)), ρ_{air} is the air density (kg m^{-3}), c_p is the specific heat at constant pressure (MJ kg^{-1} °C^{-1}; assumed to be 1.01×10^{-3} MJ kg^{-1} °C^{-1} for all simulations), e_z^o is the saturation vapor pressure of air at height z (kPa; assumed to be 2 m for all simulations), γ is the psychometric constant (kPa °C^{-1}), r_c is the plant canopy resistance (s m^{-1}) and r_a is the aerodynamic resistance (s m^{-1}). Full details of the Penman–Monteith method and the calculation of its parameters are described by Monteith (1965).

The plant canopy resistance term was modified to account for the effects of CO_2 and vapor pressure deficit on ETo (Stockle et al., 1992). r_c is calculated as:

$$r_c = (0.5 \times g_l(\mathrm{VPD}, CO_2) \times \mathrm{LAI})^{-1} \tag{18}$$

where g_l (VPD, CO_2) is the maximum conductance of a single leaf considering the effects of vapor pressure deficit and increased CO_2 (m s^{-1}). When calculating actual evapotranspiration, the canopy resistance term is modified to reflect the impact of high vapor pressure deficit on leaf conductance following the approach by Stockle et al. (1992). For a plant species, a threshold vapor pressure deficit is defined at which the plant's leaf conductance begins to drop in response to the vapor pressure deficit. The adjusted leaf conductance is calculated as:

$$\begin{aligned} g_l(\mathrm{VPD}) &= g_{l,mx} \times (1 - \Delta g_{l,dcl} \times (\mathrm{VPD} - \mathrm{VPD}_{\mathrm{thr}})) && \text{if VPD} > \mathrm{VPD}_{\mathrm{thr}} \\ g_l(\mathrm{VPD}) &= g_{l,mx} && \text{if VPD} \le \mathrm{VPD}_{\mathrm{thr}} \end{aligned} \tag{19}$$

where g_l(VPD) is the stomatal conductance accounting for the effects of a high vapor pressure deficit, $g_{l,mx}$ is the maximum stomatal conductance for a plant, according to the EPIC crop database (Williams et al., 1989), $\Delta g_{l,dcl}$ is the rate of decline in leaf conductance per unit increase in vapor pressure deficit (m s^{-1} kPa^{-1}), VPD is the vapor pressure deficit (kPa) and $\mathrm{VPD}_{\mathrm{thr}}$ is the threshold deficit above which a plant will exhibit reduced leaf conductance (kPa). $\Delta g_{l,dcl}$ is calculated:

$$\Delta g_{l,dcl} = \frac{1 - fr_{g,mx}}{\mathrm{VPD}_{fr} - \mathrm{VPD}_{\mathrm{thr}}} \tag{20}$$

where $fr_{g,mx}$ is the fraction of the maximum stomatal conductance, $g_{l,mx}$, achieved at the vapor pressure deficit VPD_{fr}. $fr_{g,mx}$ is assumed to be 0.75 and VPD_{fr} is assumed to be 4 for all scenarios, as given in the EPIC database (Williams et al., 1989).

The canopy resistance term was also modified to account for the effects of CO_2 concentration on leaf conductance following the work of Morison (1987) and Easterling et al. (1992). Morison (1987) found that at CO_2 concentrations between 330 and 660 ppm, a doubling in CO_2 concentration resulted in an average reduction of 40% in leaf conductance for various plant species. Other plants, however, may exhibit different reductions for a doubling of CO_2. For example, deciduous forest has been shown to exhibit a 24% reduction with a doubling of CO_2 (Medlyn et al., 2001). To account for these variations, conductance reduction values from the literature (Table 3) were used. Easterling et al. (1992) proposed a modification to the leaf conductance term for simulating CO_2 concentration effects on ETo. Their equation was modified to account for plant species with varying responses to increased atmospheric CO_2 concentrations:

$$g_l(\mathrm{VPD}, CO_2) = g_l(\mathrm{VPD}) \times \left((1 + \Delta_{g_l CO_2}) - \Delta_{g_l CO_2}\left(\frac{CO_2}{330}\right)\right) \tag{21}$$

where $g_l(\mathrm{VPD}, CO_2)$ is the leaf conductance term modified to reflect the effect of a high vapor pressure deficit and CO_2 concentrations, $\Delta_{g_l CO_2}$ is the conductance reduction percentage for doubling of CO_2

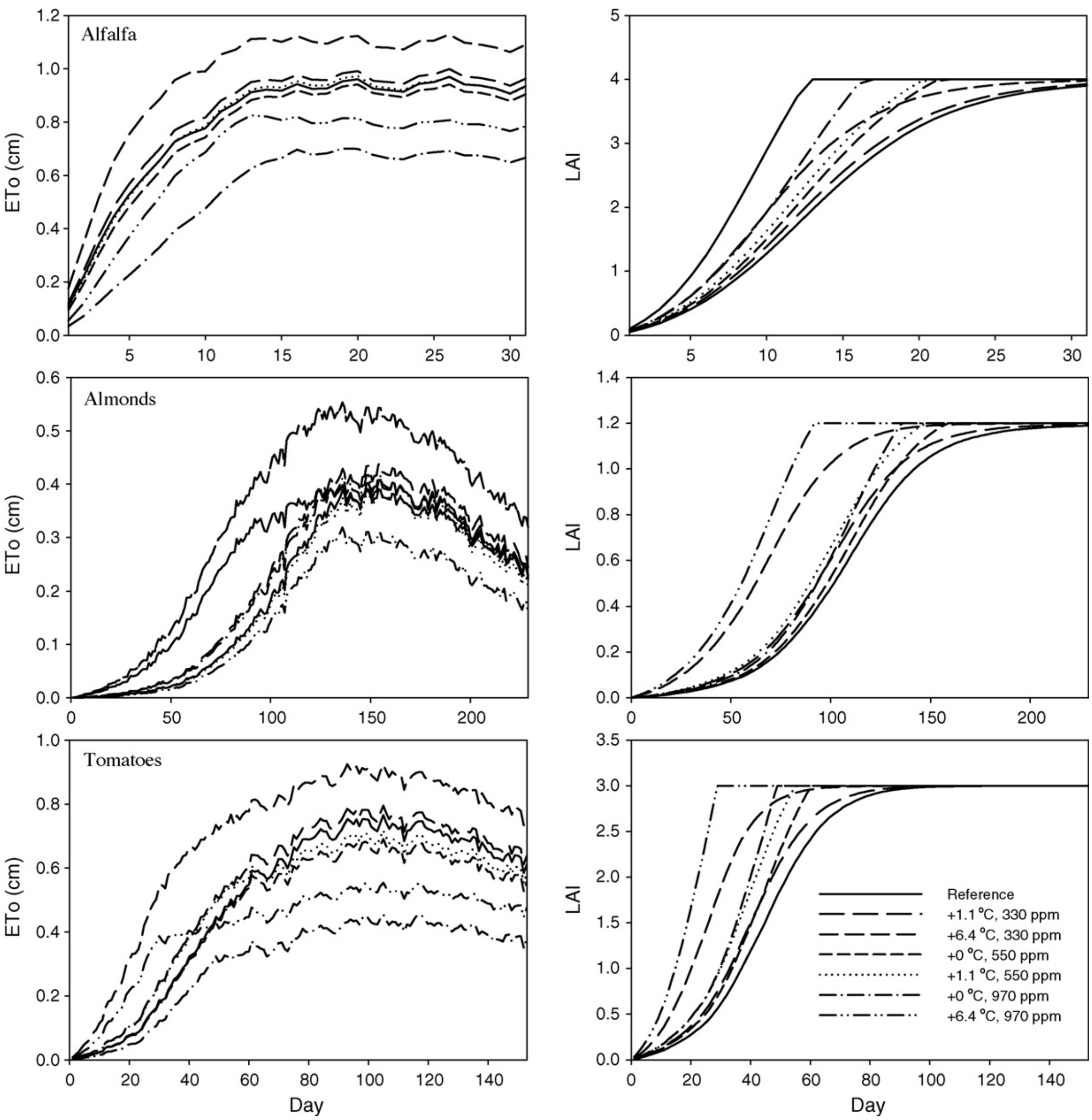

Fig. 3. Daily potential evapotranspiration and leaf area index for all crops and climate change scenarios.

(%) and CO_2 is the concentration of carbon dioxide in the atmosphere (ppm). It is assumed that the effect of CO_2 on stomatal conductance is a linear relationship (Easterling et al., 1992).

To test the ETo model, we compared it to the Davis CIMIS site from 1982 to 2009. The root mean square error between the observed and modeled ETo data was 0.52 mm/day. A *T*-test was ran at $\alpha = 0.05$ and found no significant difference between the model and CIMIS ETo data. The percent bias statistic, a measure of the average tendency of the simulated data to be larger or smaller than the observed data, was calculated and found to be −1.4%, which indicates a low model overestimation. For reference, a percent bias of ±25% can be deemed a satisfactory model at not over- or under-predicting the observed data (Moriasi et al., 2007). The sites used in this study were also found to accurately simulate CIMIS ETo. Graphical comparisons for multiple CO_2 concentrations at the Davis, CA CIMIS site are shown in Fig. 2.

It is important to reiterate that we assume the relationship between CO_2 concentration and plant transpiration will remain constant through time. This relationship may or may not stay constant depending on the adaptation/acclimation by the crops, but it is beyond the breadth of this study to determine the changes in this relationship. Previous studies have shown that the major discrepancy in this relationship can be related to changes in the tissue nitrogen content within the plant (Drake et al., 1997; Gonzalez-Meler et al., 2004). Tissue nitrogen concentration often decreases at increased CO_2 concentrations (Drake et al., 1997), and the relationship between plant transpiration and tissue nitrogen concentration is well defined. Therefore, any changes in tissue nitrogen concentration will result in changes in plant transpiration. Consequently, our assumption of a constant CO_2 concentration and plant transpiration may result in an overestimation of plant transpiration at higher CO_2 concentrations.

4.6. Root growth

Root depth was modeled using a logistic growth function in HYDRUS 1D (Šimunek et al., 2005). The modeled rooting depth was assumed to increase with time until reaching the maximum

Table 4
Changes in cumulative recharge (%) relative to the reference scenario for all climate change scenarios.

Crop	Value	Scenario						
		Reference	+1.1 °C	+6.4 °C	+0 °C, 550 ppm	+1.1 °C, 550 ppm	+0 °C, 970 ppm	+6.4 °C, 990 ppm
Alfalfa	Cumulative recharge (cm)	1.78	1.76	1.71	1.76	1.72	1.78	1.64
	Percent difference	–	−1.1	−4.0[a]	−1.1	−3.4	0	−8.4
Almonds	Cumulative recharge (cm)	21.57	21.62	18.89	21.38	21.62	20.14	21.47
	Percent difference	–	0.2	−13.2[a]	−0.9	0.2	−6.9	−0.4[a]
Tomatoes	Cumulative recharge (cm)	23.02	25.3	28.77	20.4	22.31	8.16	12.29
	Percent difference	–	9.5[a]	22.2[a]	−12.1[a]	−3.1	−95.3[a]	−60.8[a]

[a] Indicates that *T*-tests are significantly different from the reference scenario at alpha = 0.05.

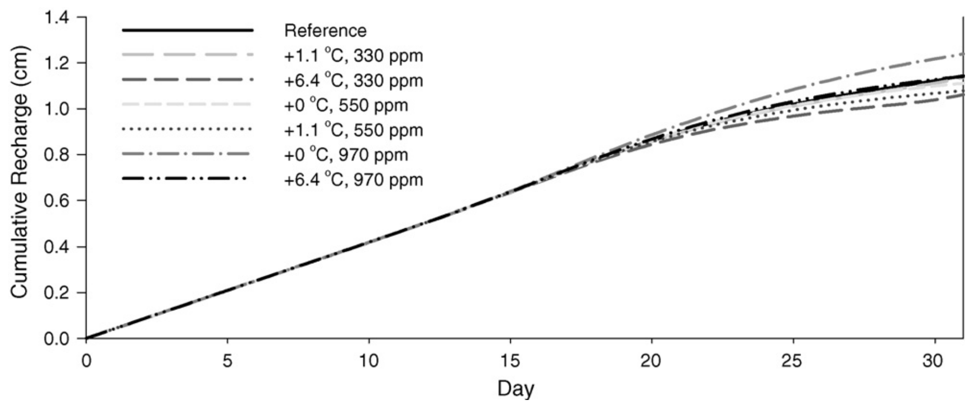

Fig. 4. Cumulative groundwater recharge for the alfalfa growing season for all climate change scenarios.

rooting depth at the end of crop development. Alfalfa and almond crops are perennial plants, and therefore the rooting depth was assumed to be the maximum rooting depth throughout the simulation. Maximum rooting depth values were derived from the EPIC crop database (Williams et al., 1989) and the United States Environmental Protection Agency (USEPA; USEPA, 2009).

5. Results

5.1. Leaf area index

LAI was affected by increases in temperature and changes in atmospheric CO_2 concentration (Fig. 3). Increasing average daily temperature by 1.1 and 6.4 °C and increases in CO_2 concentration resulted in a decrease in time to reach the crop's maximum LAI when compared to the reference scenario. This result varied depending on the crop (Fig. 3). For example, the maximum LAI of alfalfa was reached 4 days earlier with a 6.4 °C increase and 9 days earlier with an increase of CO_2 to 550 ppm. Coupling increased temperatures and CO_2 concentrations caused an even faster time to reach maximum LAI. This result varied depending on the crop. For example, an increase of CO_2 and temperature caused a faster time to reach maximum LAI by 15 days, whereas tomatoes increased by approximately 30 days.

5.2. Potential evapotranspiration

ETo was affected by increases in temperature and atmospheric CO_2 concentration (Fig. 3). Increasing temperature alone caused an increase in average daily ETo and increasing CO_2 alone decreased average daily ETo throughout the simulation time compared to the reference scenario. However, increasing temperature by 1.1 °C and an increase of CO_2 to 550 ppm led to only small decreases (0.3 mm/day for alfalfa) in average daily ETo, whereas temperature

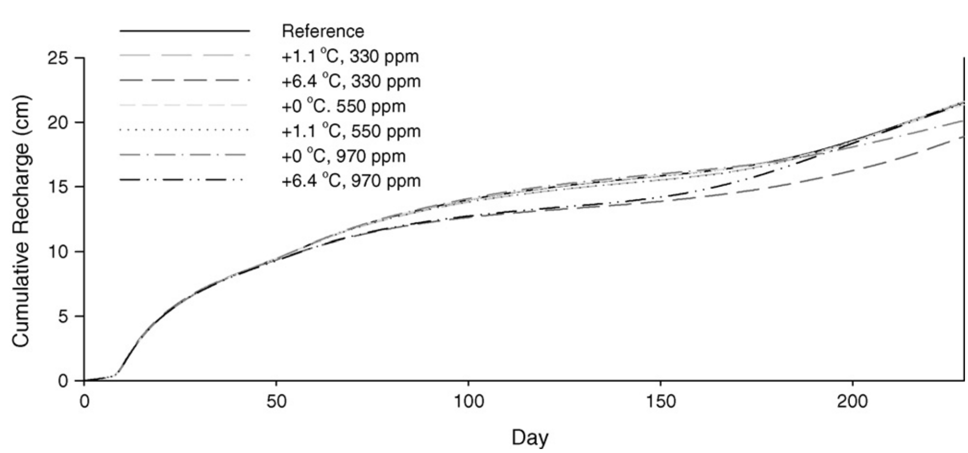

Fig. 5. Cumulative groundwater recharge for the almond growing season for all climate change scenarios.

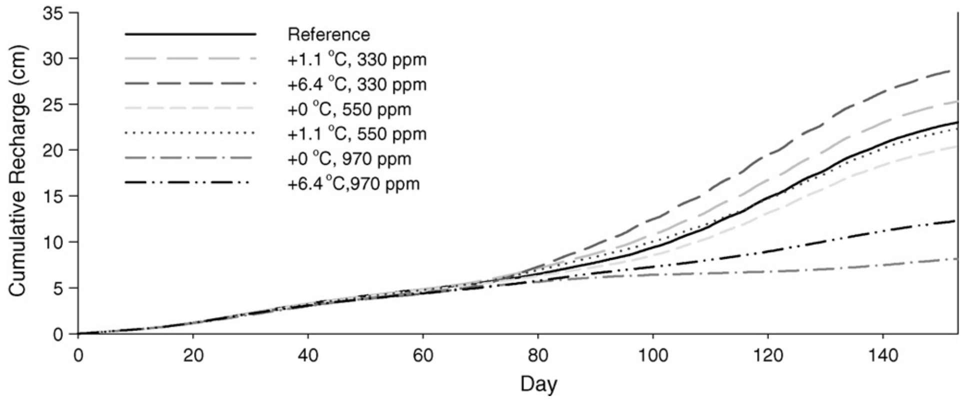

Fig. 6. Cumulative groundwater recharge for the tomato growing season for all climate change scenarios.

increases by 6.4 °C and a CO_2 concentration of 970 ppm resulted in large decreases (0.9 mm/day for alfalfa) in average daily ETo, especially for alfalfa and tomatoes. For almonds, average daily ETo under high temperature and CO_2 conditions was comparable to the reference ETo during the second half of the almond growing season.

5.3. Cumulative groundwater recharge

Considering the spatial and temporal variability in groundwater recharge due to land use, the recharge values found within the study are reasonable when compared to other groundwater recharge studies in the San Joaquin Valley that estimate a recharge rate between 7.5 and 60 cm per year under agricultural fields (Burow et al., 1999, 2008; Spurlock et al., 2000).

5.3.1. Alfalfa

Cumulative groundwater recharge of the reference scenario for one cycle of the alfalfa season (31 days) was 1.78 cm (Table 4). Cumulative recharge did not increase under any climate change scenario and did not change for an increase of CO_2 to 970 ppm compared to the reference scenario. The largest decrease in cumulative recharge compared to the reference scenario was 8.4% when temperature was increased by 6.4 °C and CO_2 to 970 ppm. It is important to note the scale of cumulative groundwater recharge for alfalfa on Fig. 4. The difference between the reference scenario and the scenario with the largest percent change was only 0.14 cm.

5.3.2. Almonds

Cumulative recharge of the reference scenario for the almond growing season (229 days) was 21.57 cm (Table 4, Fig. 5). The largest percent decrease in cumulative recharge compared to the reference scenario was 13.2% with an increase of average daily temperature by 6.4 °C. The largest percent increase was 0.2% and occurred for two scenarios: [1] solely increasing average daily temperature by 1.1 °C and [2] increased average daily temperature by 1.1 °C and CO_2 to 550 ppm.

5.3.3. Tomatoes

Cumulative recharge of the reference scenario for the tomato growing season (153 days) was 23.01 cm (Table 4, Fig. 6). Recharge increased by 9.5 and 22.2% for increases in temperature by 1.1 and 6.4 °C, respectively. The largest decrease in recharge was 95.3% and occurred when atmospheric CO_2 was increased to 970 ppm. The smallest decrease was 3.1% and occurred when temperature was increased by 1.1 °C and CO_2 to 550 ppm.

6. Discussion

Increasing average daily temperature had two effects on groundwater recharge: [1] increased ETo resulting in an increased use of irrigation water potentially available for groundwater recharge and [2] decrease in time to reach maximum LAI for the growing season resulting in increased ETo and plant water use in the earlier portion of the growing season. Recharge under tomatoes increased by 9.5 and 22.2% for an increase of 1.1 and 6.4 °C, respectively, while recharge under alfalfa and almonds generally decreased. These contrasting results can be explained by the difference in root growth under the irrigation regimes imposed during the simulation, as alfalfa and almonds are perennial crops and were simulated with constant root depths. This allows the plant to consume more water during the early growth cycles in comparison to tomatoes, whose roots are in the early stages of growth and are shallow.

Increasing atmospheric CO_2 concentration had two major effects on agriculture and groundwater recharge: [1] an increase in crop water use efficiency resulting in less water needed for irrigation and [2] increased plant growth rates resulting in more irrigation needed earlier in the growing season. The plant's water use efficiency increases with an increase in CO_2 concentration. The increase in crop water use efficiency decreases ETo rates, causing an overall decline in irrigation water use, and therefore less available water for groundwater recharge. The ETo of alfalfa did not change with respect to the reference scenario when CO_2 concentration was elevated to 970 ppm. This can be explained by the conflicting effects of increased CO_2 concentration: [1] decreasing the time to reach maximum LAI leading to increased irrigation use while also [2] increasing the water use efficiency.

Increased plant growth due to elevated CO_2 concentrations had similar effects as increased temperature, resulting in a shorter time to reach maximum LAI. In contrast, an increase in CO_2 concentration also decreased ETo rates. Morison and Gifford (1984) showed that a doubling of CO_2 concentration resulted in an increase in the plant transpiration rate in the early stages of growth due to rapid plant development. Therefore, increased rates of plant development can partially offset the decrease in stomatal conductance. However, Table 4 shows that groundwater recharge generally decreased with an increase in CO_2 concentration. One potential explanation would be that the effect of decreased ETo from increased water use efficiency may have a larger effect on groundwater recharge than increased irrigation from increased plant growth due to elevated CO_2 concentrations.

Increases in average daily temperature coupled with increases in CO_2 concentrations led to decreases in groundwater recharge for all crops. The coupling of the effects of increased average daily temperature (increased daily ETo and shorter time to maximum LAI) and increased CO_2 concentration (decreased daily ETo and decreased time to maximum LAI) makes it difficult to determine the main cause of decreased groundwater recharge. Compared to scenarios where CO_2 concentration was the only variable that increased, increasing temperature and CO_2 concentration resulted in more groundwater recharge, but still less than the reference scenario. One would expect an increase in groundwater recharge from increased irrigation due to higher ETo and plant growth. However, the coupling of increased ETo from average daily temperature and increased plant growth due to an increase in average daily temperature and CO_2 may have a larger role in determining the amount of groundwater recharge than the effect of increased water use efficiency.

The climate change scenarios were constructed to assess the sensitivity of groundwater recharge to potential future greenhouse gas emissions and climate changes. Potential sources of errors remain such as the use of global scenarios developed by the IPCC rather than region-specific scenarios, lack of information on possible changes in the amounts and intensity of precipitation and temperature extremes as well as specifications concerning other meteorological variables such as wind speed and relative humidity.

This study focuses on direct impacts of climate change on groundwater recharge but other factors may directly affect groundwater recharge under climate change. Examples include evolution of vegetation and changes in land use and agricultural management practices. One of the management practices simulated in this study, irrigation, was simulated based on plant needs. It was assumed that to maintain peak crop production, growers would irrigate so that the crop was rarely under water stress. Since groundwater recharge is a direct result of groundwater recharge during growing months, the assumption that the plant will achieve maximum growth due to unlimited water may distort the results. It is beyond the scope of this paper to determine whether irrigation demands can be met under climate change. However, the scenarios presented in the study act as a sensitivity analysis for comparison to present-day conditions, where the amount of irrigation water applied to crops is for maximum yield.

No consistent projection for California precipitation has been concluded, with different climate projections showing decreases and increases in precipitation (Cavagnaro et al., 2006), and any precipitation increases during the summer months are likely to be minimal due to the Mediterranean climate. A number of studies have concluded that, while there will be a dramatic difference in regional impacts, agricultural production in the United States overall will increase, and irrigation water use will go down to due to increased precipitation (National Assessment Synthesis Team, 2001). More importantly is the effect of climate change on the California Sierra Nevada snowpack, with predictions indicating a 30–70% lower snowpack compared to current conditions due to an earlier snowmelt. Since the snowpack is the largest contributor to California's water resources, a heavier reliance on groundwater may occur, a resource that is continually being depleted in California's Central Valley (Faunt, 2009). Therefore, the assumption that there will be an unlimited amount of water for irrigation may not hold true, and if so, a decrease in groundwater recharge may be expected.

Assuming that climate change will have a drastic effect on California's water resources, irrigation efficiency will become increasingly important. Changes in irrigation efficiency from evolving irrigation methods will have a large effect on the amount of water needed and therefore on groundwater recharge. Newly developed irrigation methods such as subsurface drip and microspray technologies have irrigation application efficiencies of approximately 90% (Howell, 2003), leading to less irrigation water used per application and therefore less available water for recharge. Precision irrigation is one of the most effective water conservation techniques and increases the efficiency of fertilizer application through fertigation with decreased potential for leaching nitrate, pesticides and other soluble agricultural chemicals (Cavagnaro et al., 2006). However, the economic cost of precision irrigation is high. These and newer techniques will become important to lessen the demand for irrigation water in a changing climate. On the other hand, increases in ETo rates will increase surface water evaporation, potentially reducing irrigation efficiency.

Because of the broad simplification of the effects of CO_2 on plant growth included and the use of multiple models, this analysis is still perhaps too uncertain for detailed water management purposes. The goal of this work is to test the sensitivity of groundwater recharge under climate change and increases in atmospheric CO_2 concentration. More work should be focused on the relationship between elevated atmospheric CO_2 concentrations and plant growth/water use efficiency. The relationships between atmospheric CO_2 concentrations and plant growth and transpiration used in this study were taken from other studies. These relationships, however, must be used with caution, as these values may differ from region to region (Morison, 1987). Although the simulations were conducted in only one dimension with many assumptions, they represent some extreme conditions and show significant effects resulting from climate change.

6.1. Implications

The modeled hydrologic changes presented in this study may have implications for agricultural and water management and groundwater quality in the Central Valley of California. A shift in irrigation timing due to changes in plant growth and a decrease in ET would cause water resource managers to change their water allotment to meet the farmers' needs. Increased recharge would allow for more agricultural pollutant transport into an already polluted groundwater system. Conversely, increased groundwater recharge would increase groundwater storage in an area where groundwater storage is needed and will continue to be increasingly important in the future.

It is likely that growers would alter their planting season to account for an increase in plant growth rates. Faster crop development occurs with higher average daily temperatures (Fig. 3) (Ritchie and NeSmith, 1991). Faster crop development may result in reduced growing season water demand, but may increase annual water demand due to the potential of multiple cropping. Therefore, simulating vadose zone processes for a constant growing season scenario could potentially alter the groundwater recharge results. For example, Fig. 3 shows that alfalfa reaches its maximum LAI approximately 10 days sooner with an increase of temperature by 1.1 °C and CO_2 to 550 ppm. It is safe to assume that the growers would therefore harvest alfalfa at an earlier date compared to the harvest date used in this study, resulting in changes to the hydrologic cycle.

7. Conclusions

The results of this study suggest that groundwater recharge in the study area may be very sensitive to increased average daily temperatures and atmospheric CO_2 concentrations. In these simulations, increasing temperature caused a temporal shift in plant growth patterns and redistributed evapotranspiration and irrigation water use earlier in the growing seasons. These shifts resulted in a decrease in groundwater recharge under alfalfa and almonds and an increase under tomatoes. Less irrigation water was needed because of a decreased evapotranspiration rate. Because a large portion of the growing season is in the summer, where precipitation is negligible, groundwater recharge is largely correlated with irrigation water use. Since there was a decrease in irrigation water use, there was also a decrease in groundwater recharge. An increase of average daily temperature by 1.1 and 6.4 °C and atmospheric CO_2 concentration to 550 and 970 ppm decreased cumulative groundwater recharge for most scenarios.

Agricultural implications resulting from this study include changes to plant growth and daily evapotranspiration rates leading to changes in groundwater recharge, both of which may affect future water resources and water quality. These modeled hydrologic changes may have implications for agricultural management and water quality in the San Joaquin Valley of California, a topic that has recently become very important (Singleton et al., 2007). A shift in irrigation timing due to changes in plant growth and a decrease in evapotranspiration might force water resource managers to change their water allotment to meet the farmers' needs. Also, with increased plant growth, the potential for the planting of multiple crops per growing seasons may occur, possibly increasing fertilization. This study points out the need for an improved understanding of the effects of increased temperature and atmospheric CO_2 concentrations on plant growth and transpiration, which could greatly reduce the uncertainty of groundwater recharge estimates in agriculturally dominated areas.

Acknowledgements

The authors would like to thank Dr. Jan Hopmans, Dr. Jirka Šimunek and Dr. Marcel Schaap for their support in learning the methods used in this study.

Appendix A. Supplementary data

Supplementary data associated with this article can be found, in the online version, at doi:10.1016/j.agwat.2010.02.009.

References

Aranjuelo, I., Irigoyen, J., Perez, P., Martinez-Carrasco, R., Sanchez-Diaz, M., 2006. Response to nodulated alfalfa to water supply, temperature and elevated CO_2: productivity and water relations. Environmental and Experimental Biology 55, 130–141.

Aranjuelo, I., Irigoyen, J., Nogues, S., Sanchez-Diaz, M., 2009. Elevated CO_2 and water-availability effect on gas exchange and nodule development in N-2-fixing alfalfa plants. Environmental and Experimental Biology 65, 18–26.

Boswell, V.G., 1926. The influence of temperature upon the growth and yield of garden peas. Proceedings of the American Society of Horticultural Science 23, 162–168.

Burow, K.R., Panshin, S.Y., Dubrovsky, N.M., Vanbrocklin, D., Fogg, G.E., 1999. Evaluation of processes affecting 1,2-dibromo-3-chloropropane (DBCP) concentrations in ground water in the eastern San Joaquin Valley, California: analysis of chemical data and ground water flow and transport simulations. U.S. Geological Survey Pub. WRI 99-4059, pp. 57.

Burow, K.R., Shelton, J.L., Dubrovsky, N.M., 2008. Regional nitrate and pesticide trends in ground water in the eastern San Joaquin Valley, California. Journal of Environmental Quality 37, S-249–S-263.

California Agriculture Resource Directory (CARD), 2009. California Department of Food and Agriculture. Available at: http://www.cdfa.ca.gov/statistics/.

California Department of Finance (CA-DOF), 2007. California's agricultural commodities: commodity ranking, acreage, production value, crop harvest seasons, and leading producing counties, 2007. Available at: http://www.dof.ca.gov/HTML/FS_DATA/STAT-ABS/documents/G13A.pdf.

California Department of Water Resources (DWR), 2003. Bulletin 118: California's Groundwater, 2003. Available at: http://www.water.ca.gov/groundwater/bulletin118/bulletin118update2003.cfm.

Cavagnaro, T., Jackson, L., Scow, K., 2006. Climate Change: challenges and solutions for California agricultural landscapes. A report from: California Climate Change Center. CEC-500-2005-189-SF.

Cross, H.Z., Zuber, M.S., 1972. Prediction of flowering dates in maize based on different methods of estimating thermal units. Agronomy Journal 26, 351–355.

Drake, B.G., Gonzalez-Meler, M.A., Long, S.P., 1997. More efficient plants: a consequence of rising atmospheric CO_2? Annual Review of Plant Physiology and Plant Molecular Biology 48, 609–639.

Easterling, W.E., Rosenberg, N.J., McKenney, M.S., Allan Jones, C., Dyke, P.T., Williams, J.R., 1992. Preparing the erosion productivity impact calculator (EPIC) model to simulate crop response to climate change and the direct effects of CO_2. Agricultural and Forest Meteorology 59, 17–34.

Eckhardt, K., Ulbrich, U., 2003. Potential impacts of climate change on groundwater recharge and streamflow in a central European low mountain range. Journal of Hydrology 284, 244–252.

Faunt, C. ed., 2009. Groundwater Availability of the Central Valley Aquifer. U.S. Geological Survey Professional Paper 1766, 225 p. Available at: http://pubs.usgs.gov/pp/1766.

Feddes, R., Kowalik, P., Zaradny, H., 1978. Simulation of Field Water Use and Crop Yield. John Wiley and Sons, NY.

Ficklin, D., Luo, Y., Luedeling, E., Zhang, M., 2009. Climate change sensitivity assessment on the San Joaquin Watershed using SWAT. Journal of Hydrology 347, 16–29, doi:10.1016/j.jhydrol.2009.05.016.

Gonzalez-Meler, M., Taneva, L., Trueman, R., 2004. Plant respiration and increased atmospheric CO_2: cellular responses and global significance. Annals of Botany 94, 647–656.

Guerra, L., Hoogenboom, G., Boken, V., Hook, J., Thomas, D., Harrison, K., 2004. Evaluation of the EPIC model for simulating crop yield and irrigation demand. Transactions of the ASAE 47, 2091–2100.

Hatfield, J., Reginato, R., Idso, S., 1984. Evaluation of canopy temperature-evapotranspiration models over various crops. Agricultural and Forest Meteorology 32, 41–53.

Howell, T.A., 2003. Irrigation Efficiency. Encyclopedia of Soil Science. Taylor & Francis, New York, NY, pp.936–949.

IPCC, 2001. Special Report on Emission Scenarios. Cambridge University Press, 612 pp.

IPCC, 2007. Climate Change 2007: The Physical Science Basis. Contribution of working group I to the fourth assessment report of the Intergovernmental Panel on Climate Change. Cambridge University Press, Cambridge, United Kingdom and New York, NY, USA.

Magoon, C.A., Culpepper, C.W., 1932. Response of sweet corn to varying temperatures from time of planting to canning maturity. USDA Technical Bulletin, 312.

Maurer, E.P., 2007. Uncertainty in hydrologic impacts of climate change in the Sierra Nevada, California, under two emission scenarios. Climatic Change 82, 309–325.

Medlyn, B., Barton, C., Broadmeadow, M., Ceulemans, R., De Angelis, P., Forstreuter, M., Freeman, M., Jackson, S., Kellomaki, S., Laitat, E., Rey, A., Roberntz, P., Sigurdsson, B., Strassemeyer, J., Wang, K., Curtis, P., Jarvis, P., 2001. Stomatal conductance of forest species after long-term exposure to elevated CO_2 concentrations: a synthesis. New Phytologist 149, 247–264.

Monteith, J.L., 1965. Evaporation and environment. In: Fogg, G.E. (Ed.), Symposium of the Society for Experimental Biology, The State and Movement of Water in Living Organisms, vol. 19. Academic Press, Inc., NY, pp. 205–234.

Moriasi, D.N., Arnold, J.G., Van Liew, M.W., Binger, R.L., Harmel, R.D., Veith, T.L., 2007. Model evaluation guidelines for systematic quantification of accuracy in watershed simulations. Transactions of the ASABE 50, 885–900.

Morison, J.L., Gifford, R.M., 1984. Plant growth and water use with limited water supply in high CO_2 concentrations. I. Leaf area, water use and transpiration. Australian Journal of Plant Physiology 11, 361–374.

Morison, J.L., 1987. Intercellular CO_2 Concentration and Stomatal Response to CO_2 Stomatal Function. Stanford University Press, Stanford California, pp. 229–251.

Mualem, Y., 1976. A new model predicting the hydraulic conductivity of unsaturated porous media. Water Resources Research 12, 513–522.

National Agricultural Statistics Service (NASS), 2009. 2009 Census of Agriculture. Available at: http://www.agcensus.usda.gov.

National Assessment Synthesis Team, 2001. Climate Change Impacts on the United States: The Potential Consequences of Climate Variability and Change. Ed C U Press, Cambridge, U.K.

Neuman, S., Feddes, R., Bresler, E., 1975. Finite element analysis of two-dimensional flow in soil considering water uptake by roots. I. Theory. Soil Science Society of America Journal 35, 224–230.

Nietsch, S.L., Arnold, J.G., Kiniry, J.R., Williams, J.R., King, K.W., 2005. Soil and Water Assessment Tool Theroretical Documentation. Version 2005. Texas Water Resource Institute, College Station, TX.

Pallas, J.E., 1965. Transpiration and stomatal opening with changes in carbon dioxide content of air. Science 147, 171.

Penman, H.L., 1948. Natural evaporation from open water, bare soil, and grass. Proceedings of the Royal Society of London A193, 120–146.

Pritchard, S.G., Rogers, H.H., Prior, S.A., Peterson, C.M., 1999. Elevated CO_2 and plant structure: a review. Global Change Biology 5, 807–837.

Richards, L.A., 1931. Capillary conduction of liquids through porous mediums. Physics 1, 313–333.

Ritchie, I.T. and NeSmith, D.S., 1991. Temperature and crop development. In: R.J. Hanks and J.T. Ritchie (eds.) Modeling Plant and Soil Systems. American Society of Agronomy Mongograph 31, Madison, WI. pp. 5–29.

Scanlon, B.R., Healy, R.W., Cook, P.G., 2002. Choosing appropriate techniques for quantifying groundwater recharge. Hydrogeology Journal 10, 18–39.

Schaap, M.G., Leij, F.J., van Genuchten, M.Th., 2001. ROSETTA: a computer program for estimating soil hydraulic parameters with hierarchical pedotransfer functions. Journal of Hydrology 241, 163–176.

Scibek, J., Allen, D., Cannon, A., Whitfield, P., 2007. Groundwater–surface water interaction under scenarios of climate change using a high-resolution transient groundwater model. Journal of Hydrology 333, 165–181.

Šimunek, J., van Genuchten, M.Th., Sejna, M., 2005. The HYDRUS-1D Software Package for Simulating the Movement of Water, Heat, and Multiple Solutes in Variably Saturated Media, Version 3.0. Department of Environmental Sciences, University of California Riverside, Riverside, California, USA, 270 pp.

Singleton, M.J., Esser, B.K., Moran, J.E., Hudson, G.B., McNab, W.W., Harter, T., 2007. Saturated zone denitrification: potential for natural attenuation of nitrate contamination in shallow groundwater under dairy operations. Environmental Science and Technology 41, 759–765.
Snyder, R., Orang, M., Bali, K., Eching, S., 2007. Basic Irrigation Scheduling. University of California Davis, Davis, CA, USA, p. 10. Available at: http://biomet.ucdavis.edu/irrigation_scheduling/bis/BIS.htm.
Spurlock, F., Burow, K., Dubrovsky, N., 2000. Chlorofluorocarbon dating of herbicide containing well waters in Fresno and Tulare Counties. Journal of Environmental Quality 29, 474–483.
Stockle, C.O., Williams, J.R., Rosenberg, N.J., Jones, C.A., 1992. A method for estimating the direct and climatic effects of rising atmospheric carbon dioxide on growth and yield of crops. Part I. Modification of the EPIC model for climate change analysis. Agricultural Systems 38, 225–238.
USDA, 2007. Soil Survey Geographic (SSURGO) Database. United States Department of Agriculture.
USEPA, 2009. California Alfalfa (Northern and Southern) Metadata, Available at: http://www.epa.gov/oppefed1/models/water/met_ca_alfalfa.htm.
van Genuchten, M.Th., 1980. A closed-form equation for predicting the hydraulic conductivity of unsaturated soils. Soil Science Society of America Journal 44, 892–898.
Vossen, P., 2008. California Climate Zones for Growing Temperate Tree Fruits and Nuts. University of California Cooperative Extension, Available at: http://homeorchard.ucdavis.edu/backyard-climate.pdf.
Wessolek, G., Asseng, S., 2006. Trade-off between wheat yield and drainage under current and climate change conditions in northeast Germany. European Journal of Agronomy 24, 333–342.
Williams, J.R., Jones, C.A., Kiniry, J.R., Spanel, D.A., 1989. The EPIC crop growth model. Transactions of the ASAE 32, 497–511.
Willits, D.H., Peet, M.M., 1989. Predicting yield response to different greenhouse CO_2 enrichment schemes—cucumbers and tomatoes. Agricultural and Forest Meteorology 44, 275–293.
Yin, J., Young, M., Yu, Z., 2008. Effects of paleoclimate and time-varying canopy structures on paleowater fluxes. Journal of Geophysical Research-Atmospheres 113, 1–14.
Zuppi, G., Sacchi, E., 2004. Hydrogeology as a climate recorder: Sahara–Sahel (North Africa) and the Po Plain (Northern Italy). Global Planet Change 40, 79–91.